An empirical investigation into predicting the volume of water accumulation in dams that supply the Metropolitan Region of Recife

Rodolfo Amorim C. da Silva[1], Rodolfo Viegas de Albuquerque[1], Milton Tavares de Melo Neto[1], João Fausto Lorenzato de Oliveira[1]

[1] [1]Programa de Pós-Graduação em Engenharia da Computação (PPGEC), Universidade de Pernambuco (UPE) – Recife – PE – Brazil
racs1@ecomp.poli.br, rva@ecomp.poli.br, milton.tavares@upe.br, fausto.lorenzato@upe.br

Abstract. *This article reports an empirical investigation on the prediction of the volume of water accumulated in dams, comparing the performance of traditional statistical methods, machine learning algorithms, and dynamic and static ensemble approaches, applied to volume time series, seeking to understand if there is any model that stands out from the others. The study showed that LSTM networks, isolated or used in ensemble, seem to be a sufficiently robust model to reproduce time series with a hydrological context.*

1. Introduction

Water stress, measured essentially by the use of water depending on the available supply, affects different parts of the world. Over 2 billion people already live in areas subject to water stress. According to independent assessments, the world will face a global water deficit of 40% by 2030. This situation will be worsened by global challenges such climate change [Water 2019].

Brazil has around 12% of the planet's freshwater available. This means that the country has one of the largest freshwater reserves in the world. However, most of this water is in the Amazon Basin, which covers a vast area of the country. This relative abundance of water resources places Brazil in a strategic position in terms of water security, but this reality is not uniform for all regions of the federation. A considerable part of the Brazilian Northeast region has historically lived with the problem of drought, especially in the region known as semi-arid, which covers nine northeastern states, most of which are located in the backlands and countryside [APAC 2015].

The state of Pernambuco, with an area of 98,067 km² and a population of 9 million inhabitants [de Geografia e Estatística IBGE 2023], has around 88.6% of its territory located in a semi-arid region, and an availability of water resources of the order of 1,270 m³ inhabitant/year, considered the lowest average of water consumed per year among Brazilian states, below the critical level indicated by the World Health Organization. 80% of the state's usable water volumes are located in the Zona da Mata and Metropolitan Recife mesoregions.

The Recife Metropolitan Region (RMR) covers an area of approximately 2,768.48 km², comprising 15 municipalities, including Recife, which is the state capital. With a population of 3.7 million people [de Geografia e Estatística IBGE 2023], it is a region supplied mainly by water dams, arranged as shown in Figure 1:

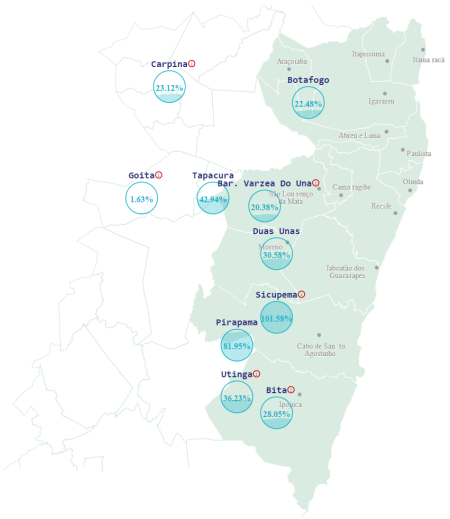

Figure 1. Illustrative example of the percentage volume accumulated in the dams that supply the Metropolitan Region of Recife (Source: COMPESA)

Considering the dependence on water dams for the regular supply of the Metropolitan Region of Recife, the predictability of the volume of water available is a fundamental data for the operational planning of the water distribution for the concessionaire which can, for example, anticipate any predicted scenario of water restriction promoting a campaign to encourage reduction in consumption and seeking alternative sources for water supply through underground water sources, desalination plants, etc. Errors in forecasting water volumes accumulated in RMR dams can cause failures in operational water distribution planning, inhibiting, for example, decision-making that seeks to mitigate water restriction scenarios.

2. Related Works

Forecasting water levels or volumes in reservoirs is a recurrent theme in hydrological and environmental studies. Different methodological families have been applied to this problem, ranging from classical statistical models to machine learning and deep learning approaches. Below, we organize the related literature into two main groups: (i) classical statistical models and (ii) machine learning and deep learning models.

2.1. Classical Statistical Models

Autoregressive models, such as AR, MA, ARMA, and their extensions with exogenous or seasonal components (e.g., ARIMAX, SARIMA, SARIMAX), have long been used in hydrological forecasting. [Sekban et al. 2022] applied these methods to monthly dam levels in Istanbul and found that an ARMA model with specific lags captured the series behavior effectively. Similarly, [Yu et al. 2017] used an ARIMA model to predict daily water levels at stations along the Yangtze River. In the context of Indian cities, [Dutta et al. 2020] used a SARIMA model to forecast reservoir levels in Chennai, highlighting its usefulness in urban water supply planning. [Reyes-Baeza et al. 2023] also employed SARIMAX for long-term forecasting of water levels in the El Yeso dam (Santiago, Chile), with promising results. [Ghimire 2017] used ARIMA models to predict daily streamflow at two stations

along the Schuylkill River in the United States, illustrating the potential of classical approaches in streamflow modeling.

2.2. Machine Learning and Deep Learning Models

Support Vector Regression (SVR) and Artificial Neural Networks (ANNs) are among the most frequently explored techniques in recent years. [Velasco et al. 2024] used SVR to predict river levels in the Philippines, demonstrating accurate short-term forecasts. MLPs (Multilayer Perceptrons) have also been applied in navigable rivers, such as in the work of [Zhou et al. 2020], who achieved reliable short- and long-term forecasts on the Nanjing section of the Yangtze River.

Recurrent neural networks, particularly LSTM models, have shown excellent performance in modeling temporal dependencies. [Widiasari et al. 2018] developed an LSTM-based flood prediction model for Semarang, Indonesia. [Hai Yen et al. 2021] proposed a multi-input LSTM using precipitation and water level data to improve forecasts for the Lai Chau dam in Vietnam. [Raman and Rathi 2024] applied LSTM models to improve dam control policies in India. Similar success with LSTM was observed by [Yang et al. 2020] for tidal levels in Taiwan and by [Fu et al. 2020] in streamflow forecasting in Malaysia.

In addition to water quantity forecasting, LSTM has also been used in related domains. [Wang et al. 2017] developed an LSTM-based model to forecast water quality parameters in Lake Taihu, China. [Lukas et al. 2024] applied MLPs to predict sedimentation levels in Ethiopia's Gibe-III reservoir based on hydrometeorological data.

3. Proposed Method

The purpose of the methodology proposed in this article is to present a complementary model to those described in the related work section, where the results of linear and non-linear models are used, individually, in the predictions. The hypothesis to be tested is that a weighted combination of a set of forecast models, which have LSTM networks in their composition, is the most appropriate approach to reproduce forecast data time series that have hydrological context, because this strategy allows us to capture simple linear patterns and more complex non-linear relationships in the data.

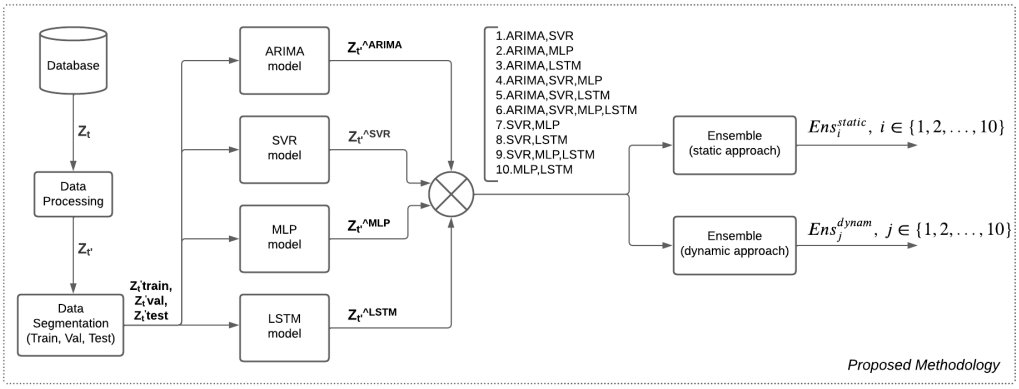

Figure 2. Proposed Methodology

As shown in Figure 2, the database (Z_t) is treated (Z'_t) and then segmented into training (Z'_{train}), validation (Z'_{val}) and testing (Z'_{test}) data. The training data (Z'_{train}) is submitted to literature models (ARIMA, SARIMA, SVR, MLP, LSTM). The validation data (Z'_{val}) is used during the training stage for tuning the hyperparameters that improve the model's performance. The selection of hyperparameters is done using the Grid Search optimization technique, according to the values described in Table 1.

Table 1. GridSearch Values

Model	Parameters	Value
ARIMA	(p, d, q)	Hyndman Method [Hyndman and Khandakar 2008]
SARIMA	(p, d, q)(P, D, Q)	Hyndman Method [Hyndman and Khandakar 2008]
SVR	**Nº Lags**	1, 2, . . . , 10
	Kernel	Linear, Poly, RBF
	Gamma	0.00001, 0.0001, 0.001, 0.01, 0.1, 1, 10, 100
	C	0.01, 0.1, 1, 10, 100
	Epsilon	0.0001, 0.001, 0.01
MLP	**Nº Lags**	1, 2, . . . , 5
	Algorithm	adam
	Activation Function	ReLU, Tanh
	Number of Hidden Layer Nodes	100
LSTM	**Algorithm**	adam
	Activation Function	ReLU
	Number of Hidden Layer Nodes	50

The linear models ARIMA and SARIMA were generated using the programming language R. The SVR model and MLP model were developed using Python 3.7 and implemented using the Sklearn library. The LSTM model was developed using Python 3.7 with the aid of Tensorflow and Keras.

The projections of the individual models are generated ($Z_t'^{ARIMA}$, $Z_t'^{SVR}$, $Z_t'^{MLP}$, $Z_t'^{LSTM}$) and subsequently combined through static and dynamic approaches, generating new predictions, this way:

1. Static approach: It was calculated the least squares solution to find the weights that minimize the sum of squares of the residuals between the specific and actual values in the data set;
2. Dynamic approach: It was implemented a dynamic combination approach that adjusts model weights based on training data, using k-NN (k-Nearest Neighbors), and these weights are used to predict target values for the test set.

The static model combination approach can be summarized in 6 steps: (I) Concatenation of predictions in the validation data, (II) Separation of variables in the validation data, (III) Calculation of Weights through the Least Squares solution (IV) Concatenation of predictions on test data, (V) Separation of variables on test data, (VI) Predictions on test set.

- Step (I) the predictions of the individual models are concatenated together with the target value (i.e. the real value) for the validation data set;
- Step (II) the predictions of the individual models (features) are separated from the actual values (labels), for the validation dataset;
- Step (III) a least squares solution is calculated to find the weights that minimize the sum of squares of the residuals between the predictions and the actual values in the validation data set;

- Step (IV) the predictions of the individual models are concatenated together with the target value (i.e. the actual value) for the test data set;
- Step (V) the individual models' predictions (features) are separated from the actual values (labels), for the test dataset.
- Step (VI) using the previously calculated weights, a test set prediction is performed by multiplying the features (individual model predictions) by the weights.

The dynamic model combination approach is structured in 5 steps: (I) Concatenation of predictions in validation data, (II) Separation of variables in validation data, (III) Concatenation of predictions in test data, (IV) Training of k-NN (k-Nearest Neighbors) on validation data, (V) Dynamic Prediction using k-NN.

- Step (I) the predictions of the individual models are concatenated together with the target value (i.e. the real value) for the validation data set;
- Step (II) the predictions of the individual models (features) are separated from the actual values (labels), for the validation dataset;
- Step (III) the predictions of the individual models are concatenated together with the target value (i.e. the actual value) for the test data set;
- Step (IV) a k-NN model is initialized with 5 nearest neighbors and the Euclidean distance metric. The model is trained with the features (individual model predictions) from the validation dataset;
- Step (V) the k-NN model is used to find the 5 nearest neighbors in the validation data based on the corresponding features. Then, a dynamic weight for these neighbors is calculated using least squares. These dynamic weights are used to predict the target value.

The performance metric adopted to systems evaluate was the MSE and MAPE. The latter, allows observing the percentage error in relation to the performance of the models.

Finally, a statistical analysis based on the Friedman test with Nemenyi post-hoc test will be carried out to evaluate the performance of the 25 models (see Table 2).

Table 2. Ensemble of Models

Individual Models	Ensemble of Models (static approach)	Ensemble of Models (dynamic approach)
ARIMA	Ens(ARIMA+SVR)(e)	Ens(ARIMA+SVR)(d)
SARIMA	Ens(ARIMA+MLP)(e)	Ens(ARIMA+MLP)(d)
SVR	Ens(ARIMA+LSTM)(e)	Ens(ARIMA+LSTM)(d)
MLP	Ens(ARIMA+SVR+MLP)(e)	Ens(ARIMA+SVR+MLP)(d)
LSTM	Ens(ARIMA+MLP+LSTM)(e)	Ens(ARIMA+MLP+LSTM)(d)
	Ens(ARIMA+SVR+MLP+LSTM)(e)	Ens(ARIMA+SVR+MLP+LSTM)(d)
	Ens(SVR+MLP)(e)	Ens(SVR+MLP)(d)
	Ens(SVR+LSTM)(e)	Ens(SVR+LSTM)(d)
	Ens(SVR+MLP+LSTM)(e)	Ens(SVR+MLP+LSTM)(d)
	Ens(MLP+LSTM)(e)	Ens(MLP+LSTM)(d)

The methodology in Figure 2 is applied to the 11 databases, and the Python Autorank package [Herbold 2020] is used to compare the performance of different forecasting models in the databases. The statistical analysis was conducted for 25 populations with 11 paired samples.

4. Experiments and Analysis

4.1. Dataset

The data set refers to the daily volume of water accumulation in water dams that supply the Metropolitan Region of Recife, in the period from 24/06/2009 to 31/12/2023, totaling 5304 records for each of the 10 dams. An eleventh database was generated, totaling the volume of accumulation available to supply the entire Metropolitan Region of Recife, through a simple sum of the volume accumulated in each of the ten dams.

During the data learning stage, the data set was subjected to a process of analysis/treatment of missing data, outlier analysis and subsequently a correlation matrix between the 10 sources was generated for understand how they relate to each other.

The eleventh time series were generated with weekly data on the accumulated volume of water, and the data was segmented into training data (60%), validation data (20%) and test data (20%).

4.2. Results and Discussion

Using MAPE and MSE as metrics to evaluate the models applied to each of the 11 datasets analyzed, the results presented in tables 6 and 7, attached at the end of the article, were obtained.

Selecting MSE as an evaluation criterion, it could be mentioned that the most accurate models were **Ens(MLP+LSTM)(d)** and **Ens(SVR+LSTM)(d)**, which obtained the best result in 3 series each (see Table 3).

Table 3. Comparison of Highest Performing Models by Dam (Ranking by MSE)

Model	1	2	3	4	5	6	7	8	9	10	11
Ens(MLP+LSTM)(d)	1º	1º	—	3º	—	2º	2º	3º	—	1º	—
Ens(ARIMA+LSTM)(d)	2º	2º	2º	2º	—	3º	1º	—	—	—	—
Ens(SVR+LSTM)(d)	3º	—	1º	1º	—	1º	—	2º	—	2º	—
Ens(ARIMA+SVR+MLP+LSTM)(e)	—	—	—	—	1º	—	—	—	1º	—	2º
Ens(SVR+MLP+LSTM)(d)	—	—	—	—	—	—	—	1º	—	—	1º
Ens(ARIMA+MLP+LSTM)(e)	—	3º	3º	—	3º	—	3º	—	2º	3º	—
LSTM	—	—	—	—	—	—	—	—	3º	—	—

Dams: 1-BITA, 2-BOTAFOGO, 3-CARPINA, 4-DUAS UNAS, 5-GOITÁ, 6-PIRAPAMA, 7-RMR (Total Sum), 8-SICUPEMA, 9-TAPACURÁ, 10-UTINGA, 11-VÁRZEA DO UNA.

Selecting MAPE as an evaluation criterion, it could be mentioned that the most accurate models were **Ens(SVR+LSTM)(d)**, **Ens(SVR+MLP+LSTM)(d)** and **LSTM**, which obtained the best result in 2 series each (see Table 4).

It is important to highlight that when analyzing the MSE and MAPE results in this tables, the best MSE values do not necessarily correspond to the best MAPE. This is due to the asymmetry of the MAPE metric [Hyndman and Koehler 2006], which evaluates positive and negative errors differently. Therefore, as MSEs perform symmetric evaluations, their values may not always be the same.

In a quick analysis, as can be seen in tables 3 and 4, the results obtained in this work suggest that, for the time series analyzed, hybrid intelligent systems built using the

Table 4. Comparison of Highest Performing Models by Dam (Ranking by MAPE)

Model	1	2	3	4	5	6	7	8	9	10	11
Ens(MLP+LSTM)(d)	1º	—	—	—	—	2º	2º	—	—	2º	—
Ens(ARIMA+MLP)(d)	—	1º	—	2º	—	—	—	—	—	—	—
LSTM	—	—	1º	—	—	—	—	—	1º	—	—
Ens(SVR+MLP)(d)	—	3º	—	1º	—	—	—	—	—	—	—
Ens(ARIMA+LSTM)(e)	—	—	—	—	1º	—	—	—	—	—	—
Ens(SVR+LSTM)(d)	2º	—	—	—	—	1º	3º	2º	—	1º	—
Ens(ARIMA+LSTM)(d)	3º	—	—	—	—	3º	1º	3º	—	3º	3º
Ens(SVR+MLP+LSTM)(d)	—	—	—	—	—	—	—	1º	—	—	1º
Ens(ARIMA+SVR)(d)	—	2º	—	3º	—	—	—	—	—	—	—
Ens(ARIMA+SVR+MLP)(e)	—	—	2º	—	—	—	—	—	—	—	—
Ens(SVR+LSTM)(e)	—	—	—	—	2º	—	—	—	—	—	—
Ens(ARIMA+MLP)(e)	—	—	—	—	3º	—	—	—	2º	—	—
Ens(ARIMA+SVR+MLP+LSTM)(d)	—	—	—	—	—	—	—	—	—	—	2º
Ens(ARIMA+SVR+MLP+LSTM)(e)	—	—	3º	—	—	—	—	—	—	—	—
Ens(ARIMA+SVR)(e)	—	—	—	—	—	—	—	—	3º	—	—

Dams: 1-BITA, 2-BOTAFOGO, 3-CARPINA, 4-DUAS UNAS, 5-GOITÁ, 6-PIRAPAMA, 7-RMR (Total Sum), 8-SICUPEMA, 9-TAPACURÁ, 10-UTINGA, 11-VÁRZEA DO UNA.

ensemble methodology seem to have better performance when compared to the results of the individual models proposed in literature.

However, a statistical analysis based on the Friedman test with Nemenyi post-hoc test will be carried out to evaluate the performance of the 25 models. Based on the decision flow of Autorank (see Figure 3) and considering we have more than two populations and some of them are not normal, it is used the non-parametric Friedman test as omnibus test to determine if there are any significant differences between the median values of the populations. It is used the post-hoc Nemenyi test to infer which differences are significant.

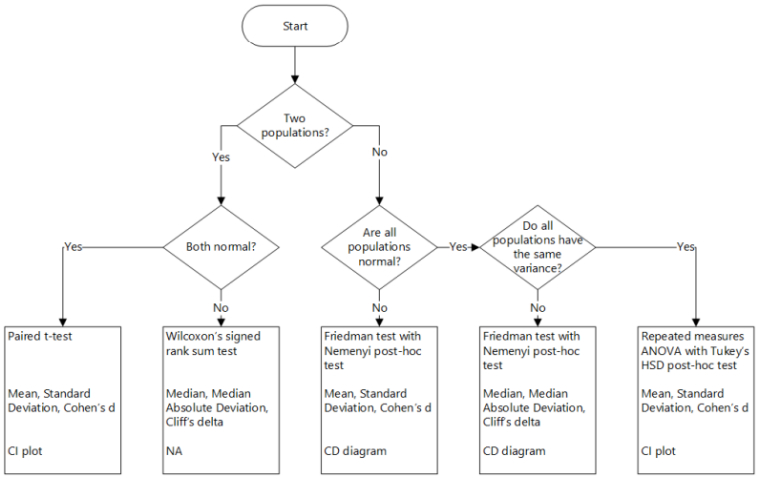

Figure 3. Decision Flow of Autorank [Herbold 2020]

It is reported the median (MED), the median absolute deviation (MAD) and the mean rank (MR) among all populations over the samples. The table 5 provides a summary of populations.

Table 5. Summary of populations

Models	MR	MED	MAD	γ	Magnitude
Ens(MLP+LSTM)(d)	3.818	7.9×10^{10}	7.9×10^{10}	0.000	negligible
Ens(SVR+LSTM)(d)	4.227	3.4×10^{10}	3.4×10^{10}	0.505	medium
Ens(ARIMA+LSTM)(d)	4.227	6.8×10^{10}	6.8×10^{10}	0.100	negligible
Ens(SVR+MLP+LSTM)(d)	6.273	2.4×10^{11}	2.4×10^{11}	−0.601	medium
Ens(ARIMA+MLP+LSTM)(d)	6.364	1.8×10^{11}	1.8×10^{11}	−0.500	small
Ens(SVR+MLP+LSTM)(e)	7.136	7.1×10^{11}	7.1×10^{11}	−0.845	large
Ens(ARIMA+MLP+LSTM)(e)	7.727	8.4×10^{11}	8.2×10^{11}	−0.876	large
Ens(ARIMA+SVR+MLP+LSTM)(e)	8.182	8.8×10^{11}	8.6×10^{11}	−0.879	large
Ens(MLP+LSTM)(e)	9.045	1.6×10^{12}	1.5×10^{12}	−0.969	large
LSTM	9.409	8.3×10^{11}	8.1×10^{11}	−0.875	large
Ens(ARIMA+LSTM)(e)	9.636	8.3×10^{11}	8.2×10^{11}	−0.863	large
Ens(ARIMA+SVR+MLP+LSTM)(d)	9.727	5.3×10^{11}	5.2×10^{11}	−0.804	large
Ens(SVR+LSTM)(e)	10.318	1.5×10^{12}	1.5×10^{12}	−0.913	large
Ens(ARIMA+MLP)(e)	16.000	3.0×10^{12}	2.9×10^{12}	−0.964	large
MLP	16.364	3.0×10^{12}	2.9×10^{12}	−0.961	large
ARIMA	17.136	3.1×10^{12}	3.0×10^{12}	−0.951	large
SARIMA	17.136	3.1×10^{12}	3.0×10^{12}	−0.951	large
Ens(SVR+MLP)(e)	17.500	3.0×10^{12}	2.9×10^{12}	−0.961	large
Ens(ARIMA+SVR+MLP)(e)	17.500	3.0×10^{12}	2.8×10^{12}	−0.988	large
SVR	17.818	3.0×10^{12}	2.9×10^{12}	−0.958	large
Ens(ARIMA+SVR)(e)	17.909	3.1×10^{12}	3.0×10^{12}	−0.961	large
Ens(ARIMA+MLP)(d)	21.364	1.5×10^{13}	1.3×10^{13}	−1.033	large
Ens(SVR+MLP)(d)	22.545	6.4×10^{12}	6.1×10^{12}	−0.982	large
Ens(ARIMA+SVR)(d)	22.909	1.3×10^{13}	1.2×10^{13}	−1.043	large
Ens(ARIMA+SVR+MLP)(d)	24.727	1.6×10^{13}	1.5×10^{13}	−1.012	large

Differences between populations are significant if the difference of the mean rank is greater than the critical distance CD=11.480 of the Nemenyi test. Based on the post-hoc Nemenyi test, we assume that there are no significant differences within the following groups (see in the critical distance diagram of Figure 4):

- Ens(MLP+LSTM)(d)
- Ens(SVR+LSTM)(d)
- Ens(ARIMA+LSTM)(d)
- Ens(SVR+MLP+LSTM)(d)
- Ens(ARIMA+MLP+LSTM)(d)
- Ens(SVR+MLP+LSTM)(e)
- Ens(ARIMA+MLP+LSTM)(e)
- Ens(ARIMA+SVR+MLP+LSTM)(e)
- Ens(MLP+LSTM)(e)
- LSTM
- Ens(ARIMA+LSTM)(e)
- Ens(ARIMA+SVR+MLP+LSTM)(d)
- Ens(SVR+LSTM)(e)

5. Conclusion

Unlike most studies that focus on individual models, this work investigates a diverse ensemble framework applied to real and sensitive data from the volume of water accumulation in dams. Although no novel algorithm is proposed, the strength of this study lies in

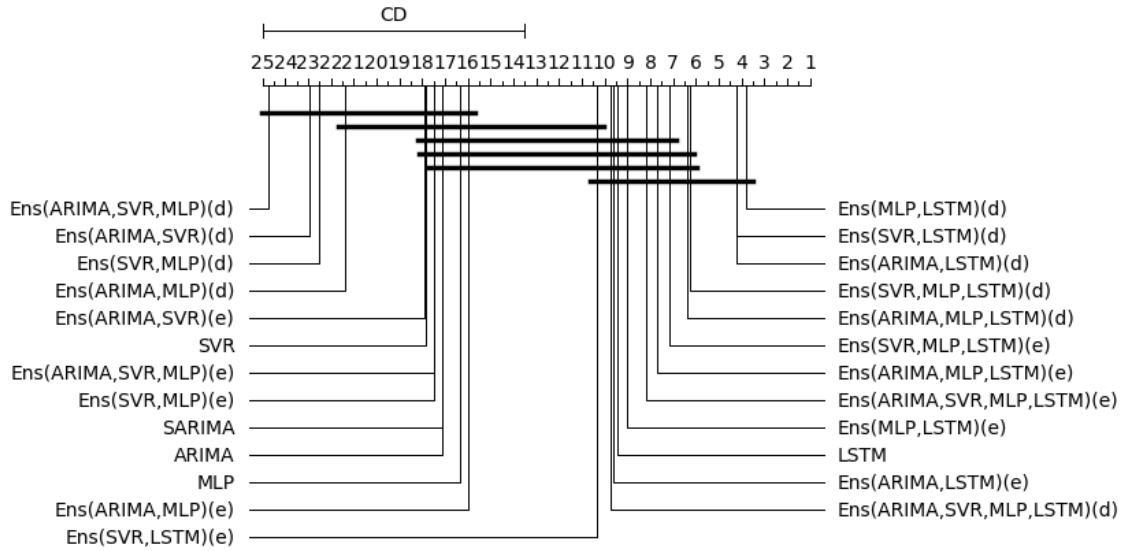

Figure 4. Critical Distance Diagram

its comparative and methodological depth, combining both static and dynamic ensemble strategies to assess predictive performance across 25 configurations.

The hybrid systems proposed here, built using ensemble techniques and tested on 11 time series of water volume accumulated in the RMR dams, outperformed classical models such as SVR, MLP, ARIMA, and SARIMA. Notably, the LSTM model, even when used in isolation, demonstrated statistically similar performance to most ensemble configurations. This suggests that LSTM networks—whether standalone or integrated in hybrid systems—are robust and reliable models for hydrological time series forecasting.

From a practical standpoint, the trade-off between performance improvement and the increased computational and modeling complexity introduced by ensemble strategies suggests that, in many operational contexts, a well-tuned LSTM model may offer a more efficient and effective solution.

A key limitation of this study is the use of univariate time series only, without exogenous variables. This choice simplifies the modeling process but may reduce interpretability and ignore relevant contextual influences. Future work could integrate additional explanatory data, such as rainfall, streamflow, or dam operation schedules, to enhance realism and generalizability. Further directions include multi-step forecasting scenarios, experiments with uncertainty estimation, and alternative ensemble selection methods.

6. Data and Code Availability

The source code used for model training and evaluation is available in a public GitHub repository: `https://github.com/racs1/source_codes-dams-RMR.git`. Due to data access restrictions, the original datasets cannot be shared publicly; however, synthetic samples and relevant metadata can be provided upon request to support replication efforts.

Table 6. Comparison of Results (using MAPE)

Model	1	2	3	4	5	6	7	8	9	10	11
ARIMA	12,5%	4,9%	8,6%	27,7%	14,2%	8,7%	3,2%	6,4%	4,2%	6,2%	4,9%
SARIMA	12,5%	4,9%	8,6%	27,7%	14,2%	8,7%	3,2%	6,4%	4,2%	6,2%	4,9%
SVR	11,7%	5,5%	16,2%	8,0%	14,1%	2,1%	5,4%	7,6%	4,2%	6,7%	4,8%
MLP	12,9%	4,6%	8,0%	9,1%	23,3%	2,5%	3,8%	8,5%	5,5%	6,0%	4,8%
LSTM	12,4%	7,8%	11,0%	6,8%	19,6%	1,9%	3,0%	2,7%	10,7%	5,3%	14,7%
Ens(ARIMA+SVR)(e)	11,9%	6,2%	15,8%	8,7%	14,3%	2,1%	5,8%	9,7%	4,1%	6,6%	5,1%
Ens(ARIMA+SVR)(d)	20,6%	14,3%	75,8%	16,8%	16,2%	7,1%	27,6%	17,6%	7,3%	9,9%	13,8%
Ens(ARIMA+MLP)(e)	12,4%	4,5%	4,9%	8,0%	13,8%	2,4%	3,1%	10,3%	4,0%	6,1%	4,9%
Ens(ARIMA+MLP)(d)	13,9%	11,6%	16,5%	15,2%	20,6%	4,8%	5,7%	47,0%	5,8%	8,5%	13,6%
Ens(ARIMA+LSTM)(e)	11,7%	5,9%	7,6%	6,0%	11,9%	1,6%	2,5%	3,0%	6,7%	4,1%	5,0%
Ens(ARIMA+LSTM)(d)	1,6%	3,8%	4,1%	2,6%	3,7%	0,3%	1,2%	0,2%	6,0%	1,9%	1,3%
Ens(ARIMA+SVR+MLP)(e)	11,9%	6,4%	12,7%	7,4%	14,2%	2,2%	5,7%	16,5%	4,3%	6,5%	5,3%
Ens(ARIMA+SVR+MLP)(d)	26,7%	27,3%	511,3%	19,5%	20,1%	7,7%	34,4%	19,2%	9,2%	10,3%	18,2%
Ens(ARIMA+MLP+LSTM)(e)	11,7%	5,8%	7,3%	6,5%	9,0%	1,6%	2,6%	2,7%	5,3%	3,2%	5,0%
Ens(ARIMA+MLP+LSTM)(d)	2,5%	3,9%	4,0%	2,2%	4,6%	0,4%	1,4%	4,1%	4,8%	2,9%	4,9%
Ens(ARIMA+SVR+MLP+LSTM)(e)	10,9%	6,0%	13,1%	6,0%	7,9%	1,6%	4,3%	10,1%	4,4%	3,2%	1,4%
Ens(ARIMA+SVR+MLP+LSTM)(d)	4,6%	8,8%	62,4%	2,5%	5,2%	0,8%	1,9%	0,4%	5,0%	4,7%	0,6%
Ens(SVR+MLP)(e)	11,8%	5,3%	13,3%	8,1%	14,4%	2,1%	5,7%	9,6%	4,3%	6,6%	4,7%
Ens(SVR+MLP)(d)	17,9%	21,1%	334,8%	13,0%	19,6%	3,9%	28,9%	12,3%	6,7%	9,3%	7,6%
Ens(SVR+LSTM)(e)	11,4%	5,8%	5,0%	5,6%	12,1%	1,9%	3,8%	2,9%	6,3%	4,6%	5,9%
Ens(SVR+LSTM)(d)	1,4%	3,9%	2,6%	2,5%	4,8%	0,3%	1,4%	0,2%	6,0%	1,5%	1,7%
Ens(SVR+MLP+LSTM)(e)	11,1%	5,9%	16,1%	3,8%	7,2%	1,8%	4,2%	2,0%	5,6%	3,7%	1,4%
Ens(SVR+MLP+LSTM)(d)	2,0%	6,0%	133,1%	3,3%	3,9%	0,5%	1,6%	0,0%	4,9%	3,1%	0,2%
Ens(MLP+LSTM)(e)	11,8%	5,6%	7,2%	4,9%	9,0%	1,8%	2,5%	2,9%	5,5%	3,4%	5,6%
Ens(MLP+LSTM)(d)	1,1%	3,4%	4,5%	3,0%	3,9%	0,3%	1,3%	0,2%	5,9%	1,8%	1,7%

Dams: 1-BITA, 2-BOTAFOGO, 3-CARPINA, 4-DUAS UNAS, 5-GOITÁ, 6-PIRAPAMA, 7-RMR (Total Sum), 8-SICUPEMA, 9-TAPACURÁ, 10-UTINGA, 11-VÁRZEA DO UNA

Table 7. Comparison of Results (using MSE) with Model Abbreviations

Model	1	2	3	4	5	6	7	8	9	10	11
ARIMA	7.18e+10	3.06e+12	1.08e+14	3.07e+12	1.88e+13	2.06e+13	2.50e+14	9.96e+10	9.23e+13	4.96e+11	1.79e+11
SARIMA	7.18e+10	3.06e+12	1.08e+14	3.07e+12	1.88e+13	2.06e+13	2.50e+14	9.96e+10	9.23e+13	4.96e+11	1.79e+11
SVR	7.23e+10	3.04e+12	7.03e+13	1.66e+12	2.31e+13	4.89e+12	4.27e+14	9.37e+10	9.15e+13	5.11e+11	2.01e+11
MLP	7.59e+10	2.99e+12	4.15e+13	1.30e+12	1.93e+13	5.49e+12	2.65e+14	1.03e+11	8.29e+13	4.14e+11	1.98e+11
LSTM	1.54e+10	8.26e+11	9.93e+12	3.42e+11	2.95e+12	1.42e+12	3.83e+13	3.58e+09	3.94e+13	1.20e+11	4.86e+11
E1	7.25e+10	3.07e+12	6.97e+13	1.60e+12	2.32e+13	4.71e+12	4.83e+14	1.01e+11	9.14e+13	5.06e+11	1.84e+11
E2	1.60e+11	1.29e+13	6.79e+14	1.15e+13	2.27e+13	2.09e+13	1.18e+16	7.56e+11	1.05e+14	1.25e+12	1.17e+12
E3	7.36e+10	2.97e+12	3.98e+13	1.29e+12	1.81e+13	5.42e+12	2.60e+14	1.10e+11	9.19e+13	4.84e+11	1.85e+11
E4	8.79e+10	3.55e+12	2.09e+14	8.94e+12	2.34e+13	2.61e+13	4.25e+14	1.45e+13	8.89e+13	7.26e+11	1.18e+12
E5	1.61e+10	1.92e+12	9.89e+12	1.19e+11	3.55e+12	8.27e+11	3.90e+13	3.76e+09	5.85e+13	1.79e+11	1.18e+11
E6	6.85e+07	9.09e+11	1.57e+12	1.86e+10	1.44e+12	4.12e+10	2.20e+13	6.11e+07	7.45e+13	6.82e+10	9.38e+09
E7	7.25e+10	3.02e+12	5.22e+13	1.44e+12	2.35e+13	4.75e+12	4.76e+14	6.25e+11	8.96e+13	4.99e+11	1.83e+11
E8	2.77e+11	1.42e+13	2.88e+16	1.62e+13	2.44e+13	3.69e+13	1.74e+16	1.00e+12	1.21e+14	1.06e+12	1.50e+12
E9	1.61e+10	1.72e+12	9.26e+12	1.22e+11	1.46e+12	8.35e+11	4.53e+13	7.71e+09	3.83e+13	4.80e+10	1.18e+11
E10	2.23e+08	6.63e+11	1.85e+12	8.32e+10	1.31e+12	9.87e+10	2.32e+13	1.82e+11	4.59e+13	1.08e+11	1.53e+11
E11	1.43e+10	1.75e+12	2.31e+13	1.12e+11	5.10e+11	8.78e+11	1.54e+14	9.27e+11	2.78e+13	4.85e+10	6.76e+09
E12	1.04e+10	4.40e+12	4.30e+14	1.01e+11	1.62e+12	5.26e+11	4.48e+13	1.64e+09	4.74e+13	4.27e+11	6.09e+09
E13	7.29e+10	2.98e+12	5.53e+13	1.43e+12	2.37e+13	4.84e+12	4.66e+14	1.01e+11	8.98e+13	5.00e+11	1.88e+11
E14	1.27e+11	5.92e+12	1.26e+16	6.39e+12	5.47e+13	8.64e+12	1.22e+16	2.61e+11	9.99e+13	8.35e+11	3.02e+11
E15	1.54e+10	1.89e+12	8.92e+12	1.96e+11	6.10e+12	1.54e+12	1.17e+14	3.63e+09	5.28e+13	2.00e+11	1.31e+11
E16	1.03e+08	9.87e+11	7.08e+11	1.17e+10	1.83e+12	3.36e+10	3.10e+13	5.03e+07	7.47e+13	2.41e+10	8.56e+09
E17	1.54e+10	1.77e+12	2.30e+13	1.11e+11	6.64e+12	8.61e+11	1.07e+14	6.23e+09	4.93e+13	2.14e+11	1.03e+11
E18	1.06e+08	1.56e+12	1.04e+14	4.18e+11	6.95e+12	8.67e+11	6.10e+13	4.58e+09	8.24e+13	3.50e+11	1.49e+11

E1:Ens(ARIMA+SVR)(e); E2:Ens(ARIMA+SVR)(d); E3:Ens(ARIMA+MLP)(e); E4:Ens(ARIMA+MLP)(d); E5:Ens(ARIMA+LSTM)(e); E6:Ens(ARIMA+LSTM)(d); E7:Ens(ARIMA+SVR+MLP)(e); E8:Ens(ARIMA+SVR+MLP)(d); E9:Ens(ARIMA+MLP+LSTM)(e); E10:Ens(ARIMA+MLP+LSTM)(d); E11:Ens(ARIMA+SVR+MLP+LSTM)(e); E12:Ens(ARIMA+SVR+MLP+LSTM)(d); E13:Ens(SVR+MLP)(e); E14:Ens(SVR+MLP)(d); E15:Ens(SVR+LSTM)(e); E16:Ens(SVR+LSTM)(d); E17:Ens(SVR+MLP+LSTM)(e); E18:Ens(SVR+MLP+LSTM)(d);

Dams: 1-BITA, 2-BOTAFOGO, 3-CARPINA, 4-DUAS UNAS, 5-GOITÁ, 6-PIRAPAMA, 7-RMR, 8-SICUPEMA, 9-TAPACURÁ, 10-UTINGA, 11-VÁRZEA DO UNA.

References

APAC, A. P. d. e. C. (2015). *Elaboração de Planos de Aproveitamento da Infraestrutura Hídrica do Semiárido - Diagnóstico da Situação Atual das Barragens e Reservatórios*, volume 01 of *Infraestrutura hídrica - Semiárido*. APAC, Agência Pernambucana de Águas e Clima, Recife/PE, Brasil.

de Geografia e Estatística IBGE, I. B. (2023). Mapeamento ibge - estado de pernambuco.

Dutta, A., Chakrabarti, A., and Gautam, J. (2020). Application of sarima for prediction of water storage levels for a metropolitan area: Chennai, a case study. In *2020 International Symposium on Advanced Electrical and Communication Technologies (ISAECT)*, pages 1–8. IEEE.

Fu, M., Fan, T., Ding, Z., Salih, S. Q., Al-Ansari, N., and Yaseen, Z. M. (2020). Deep learning data-intelligence model based on adjusted forecasting window scale: Application in daily streamflow simulation. *IEEE Access*, 8:32632–32651.

Ghimire, B. N. (2017). Application of arima model for river discharges analysis. *Journal of Nepal Physical Society*, 4(1):27.

Hai Yen, T. T., Xuan An, N., Dat, N. Q., and Solanki, V. K. (2021). Multi-input lstm for water level forecasting in black river at the border of vietnam-china. In *2021 IEEE International Conference on Machine Learning and Applied Network Technologies (ICMLANT)*, pages 1–5. IEEE.

Herbold, S. (2020). Autorank: A python package for automated ranking of classifiers. *Journal of Open Source Software*, 5(48):2173.

Hyndman, R. J. and Khandakar, Y. (2008). Automatic time series forecasting: The forecast package for r. *Journal of Statistical Software*, 27(3).

Hyndman, R. J. and Koehler, A. B. (2006). Another look at measures of forecast accuracy. *International Journal of Forecasting*, 22(4):679–688.

Lukas, P., Melesse, A. M., and Kenea, T. T. (2024). Predicting reservoir sedimentation using multilayer perceptron – artificial neural network model with measured and forecasted hydrometeorological data in gibe-iii reservoir, omo-gibe river basin, ethiopia. *Journal of Environmental Management*, 359:121018.

Raman, R. and Rathi, T. (2024). Efficient dam water level management using cloud-based data analytics and lstm networks. In *2024 11th International Conference on Reliability, Infocom Technologies and Optimization (Trends and Future Directions) (ICRITO)*, pages 1–6. IEEE.

Reyes-Baeza, P., Trujillo-Guiñez, R., and Vidal, M. (2023). Long-term water level forecasting for el yeso reservoir using time-series data and satellite images. In *2023 42nd IEEE International Conference of the Chilean Computer Science Society (SCCC)*, pages 1–7. IEEE.

Sekban, J., Nabil, M. O. M., Alsan, H. F., and Arsan, T. (2022). Istanbul dam water levels forecasting using arima models. In *2022 Innovations in Intelligent Systems and Applications Conference (ASYU)*, pages 1–7. IEEE.

Velasco, L. C., Estose, A. J., Opon, M., Tabanao, E., and Apdian, F. (2024). Performance evaluation of support vector regression machine models in water level forecasting. *Procedia Computer Science*, 234:436–447.

Wang, Y., Zhou, J., Chen, K., Wang, Y., and Liu, L. (2017). Water quality prediction method based on lstm neural network. In *2017 12th International Conference on Intelligent Systems and Knowledge Engineering (ISKE)*, pages 1–5. IEEE.

Water, U. W. (2019). *The United Nations world water development report 2021: valuing water*. Water Politics. UNESCO World Water Assessment Programmer.

Widiasari, I. R., Nugoho, L. E., Widyawan, and Efendi, R. (2018). Context-based hydrology time series data for a flood prediction model using lstm. In *2018 5th International Conference on Information Technology, Computer, and Electrical Engineering (ICITACEE)*, pages 385–390. IEEE.

Yang, C.-H., Wu, C.-H., and Hsieh, C.-M. (2020). Long short-term memory recurrent neural network for tidal level forecasting. *IEEE Access*, 8:159389–159401.

Yu, Z., Lei, G., Jiang, Z., and Liu, F. (2017). Arima modelling and forecasting of water level in the middle reach of the yangtze river. In *2017 4th International Conference on Transportation Information and Safety (ICTIS)*, pages 172–177. IEEE.

Zhou, T., Jiang, Z., Liu, X., and Tan, K. (2020). Research on the long-term and short-term forecasts of navigable river's water-level fluctuation based on the adaptive multilayer perceptron. *Journal of Hydrology*, 591.